Sensors and Materials, Vol. 30, No. 8 (2018) 1911–1918
MYU Tokyo

S & M 1649

Chaotic Motion of Double-walled Carbon Nanotubes with Fluid

Tai-Ping Chang*

Department of Construction Engineering, National Kaohsiung University of Science and Technology,
1 University Road, Yanchao, Kaohsiung, 824, Taiwan

(Received March 20, 2017; accepted June 27, 2018)

Keywords: double-walled carbon nanotubes (DWCNTs), chaotic motion, fluid-loaded, nonlinear vibration

In this study, we investigate the chaotic motion of double-walled carbon nanotubes (DWCNTs) with fluid by dealing with the effects of nonlinearities. The governing equations of the system are derived and solved by the variation method with Galerkin's technique. A chaotic phenomenon occurs when the top Lyapunov exponent of the system becomes positive. Referring to the results of the computations of the largest Lyapunov exponent, we examine and discuss the effects of some parameters, such as flow velocity, driving frequency, and load amplitude, on the chaotic motion of the nonlinear system. These parameters play an important role in determining whether or not chaotic motion will occur on the system. Moreover, these parameters can be used to control the chaos of DWCNTs conveying fluid.

1. Introduction

Carbon nanotubes (CNTs) have been utilized in numerous applications in many fields after the publication of a pioneer paper by Iijima.[1] One of their applications is as nanopipes conveying fluids.[2–5] Recently, many researchers have been studying the characteristics of nanotube vibration,[6–9] and have investigated, among others, nonlinear vibration problems with nonlocal continuum theories.[10–15] In the past, much research has been reported on the chaotic behaviors of nonlinear systems;[16–19] however, investigations about the chaotic behavior of double-walled carbon nanotubes (DWCNTs) with fluid are rare. The chaotic motion is primarily generated thanks to the nonlinear characteristics in the physical system. Here, we examine the chaotic motion of DWCNTs with fluid by studying the nonlinear characteristics. With the use of the variation method and Galerkin's technique, the governing equations of the system are derived and solved. The chaotic phenomenon occurs when the top Lyapunov exponent of the system becomes positive, as previously described.[20,21] The goal of the study is to determine whether or not the system of DWCNTs undergoes chaotic motion by computing the largest Lyapunov exponent of the system.

*Corresponding author: e-mail: tpchang@ccms.nkfust.edu.tw
http://dx.doi.org/10.18494/SAM.2018.2012

ISSN 0914-4935
http://myukk.org/

2. Simple Model for DWCNTs with Fluid

In Fig. 1, the DWCNT is modeled as a double-tube pipe composed of an inner tube of radius R_1 and an outer tube of radius R_2. The thickness of each tube is h, the length is L, and Young's modulus of elasticity is E. The internal fluid is assumed to flow steadily through the inner tube at a constant velocity U. In addition, the boundary condition of the DWCNT is assumed to be simply supported at both ends. Following the assumptions and derivations of Chang,[12] after some lengthy formulations, we obtain the governing equations for the system as follows:

$$\begin{aligned} & EI_1\frac{\partial^4 w_1}{\partial x^4} + MU^2\frac{\partial^2 w_1}{\partial x^2} - \int_0^L \left(\frac{\partial w_1}{\partial x}\right)^2\left(\frac{EA_1}{2L}+\frac{MU^2}{2L}\right)dx\frac{\partial^2 w_1}{\partial x^2} \\ & + \frac{3MU^2}{2}\left(\frac{\partial w_1}{\partial x}\right)^2\frac{\partial^2 w_1}{\partial x^2} + (M+m_1)\frac{\partial^2 w_1}{\partial \bar{t}^2} + 2MU\frac{\partial^2 w_1}{\partial x \partial \bar{t}} \\ & - MU\frac{\partial w_1}{\partial \bar{t}}\frac{\partial w_1}{\partial x}\frac{\partial^2 w_1}{\partial x^2} - c_1(w_2-w_1) - c_3(w_2-w_1)^3 = 0, \end{aligned} \tag{1}$$

$$\begin{aligned} & EI_2\frac{\partial^4 w_2}{\partial x^4} + 2\xi\frac{\partial w_2}{\partial \bar{t}} + m_2\frac{\partial^2 w_2}{\partial \bar{t}^2} - \int_0^L \left(\frac{\partial w_2}{\partial x}\right)^2\left(\frac{EA_2}{2L}\right)dx\frac{\partial^2 w_2}{\partial x^2} \\ & + c_1(w_2-w_1) + c_3(w_2-w_1)^3 = F_0\cos(\bar{\Omega}\bar{t}), \end{aligned} \tag{2}$$

where x is the axial coordinate, $\bar{t}$ is the time, w_i is the transverse displacement of the ith tube on the neutral axis, and the subscript i = 1 or 2. Note that tube 1 is the inner tube while tube 2 is the outer tube. A_1 and A_2 are the cross-sectional areas of tubes 1 and 2, respectively. I_i and m_i are the moment of inertia and the mass of the ith tube per unit length, respectively; M denotes the fluid mass. c_1 and c_3 are the van der Waals (vdW) force coefficients and are assumed to be c_1 = 71.11 GPa and $c_3 = 2.57 \times 10^4$ GPa nm^2.[22] ξ is the damping coefficient, F_0 is the magnitude of the external load, and $\bar{\Omega}$ is the driving frequency of the excitation. On the basis of Galerkin's approach, for simplicity, one term approximation is used to calculate the displacement for the nonlinear coupled system. Then, the displacement function can be expressed as

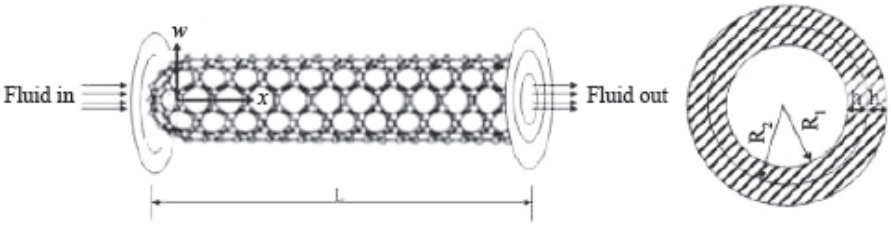

Fig. 1. Simple model for DWCNTs with fluid.

$$w_i(x,\bar{t}) = \phi(x)\bar{T}_i(\bar{t}), \tag{3}$$

where i = 1 or 2. $\phi(x)$ defines the mode shape satisfying the boundary conditions.

Equation (3) is substituted into Eqs. (1) and (2), followed by multiplication with $\phi(x)$ and integration from 0 to L. For convenience, the following dimensionless parameters are adopted to deal with the tiny values in nanosystems:

$$t = \frac{\bar{t}}{1/\omega_0} = \bar{t}w_0, \quad T_i = \frac{\bar{T}_i}{R_1}, \quad i = 1,2. \tag{4}$$

Here, $1/\omega_0$ is chosen as the characteristic time, ω_0 is the fundamental natural frequency, and R_1 is the inner tube radius, which is selected as the characteristic length. Finally, the following dimensionless differential equations can be obtained:

$$\ddot{T}_1 + a_1\dot{T}_1 + b_1T_1 + \bar{C}_1T_2 + d_1T_1^3 + e_1T_2^2T_1 + f_1T_2T_1^2 + g_1T_2^3 = 0, \tag{5}$$

$$\ddot{T}_2 + a_2\dot{T}_2 + b_2T_1 + c_2T_2 + d_2T_2^3 + e_2T_2^2T_1 + f_2T_2T_1^2 + g_2T_1^3 = F\cos(\Omega t), \tag{6}$$

where "˙" denotes $\frac{d}{dt}$. The coefficients are explicitly written in Appendix A.

3. Chaotic Motion of DWCNTs with Fluid

To study the chaotic behavior of the coupled equations, Eqs. (5) and (6), it is convenient to use the following variables: $y_1 = T_1$, $y_2 = \dot{T}_1$, $y_3 = T_2$, $y_4 = \dot{T}_2$. Then Eqs. (5) and (6) become

$$\begin{aligned}
\dot{y}_1 &= y_2,\\
\dot{y}_2 &= -a_1y_2 - b_1y_1 - \bar{C}_1y_3 - d_1y_1^3 - e_1y_3^2y_1 - f_1y_3y_1^2 - g_1y_3^3,\\
\dot{y}_3 &= y_4,\\
\dot{y}_4 &= -a_2y_4 - b_2y_1 - c_2y_3 - d_2y_3^3 - e_2y_3^2y_1 - f_2y_3y_1^2 - g_2y_1^3 + F\cos(\Omega t).
\end{aligned} \tag{7}$$

We must determine whether the above system exhibits chaotic behavior by calculating the top Lyapunov exponent. Lyapunov exponents provide an estimate of the rate of divergence of two initially nearby orbits (or trajectories), as stated in Ref. 20.

Equation (7) can be tranformed into a vector form,

$$\dot{\boldsymbol{Y}} = \boldsymbol{h}(\boldsymbol{Y}; s), \tag{8}$$

where $\boldsymbol{Y} = [y_1, y_2, y_3, y_4]^{\mathrm{T}}$ is the state-space vector, and $\boldsymbol{h} = [h_1, h_2, h_3, h_4]^{\mathrm{T}}$ and $s = (a_1, ..., g_2, F, \Omega)$ are parameters. The equations for small deviations $\delta\boldsymbol{Y}$ from the trajectory $\boldsymbol{Y}(t)$ are

$$\delta\dot{\boldsymbol{Y}} = J_{ij}(\boldsymbol{Y}(t))\delta\boldsymbol{Y}, \quad i, j = 1,2,3,4, \tag{9}$$

where $J_{ij} = \partial h_i / \partial y_j$ denotes the Jacobian matrix of derivatives.

Equation (9) for the system Eq. (7) can be rewritten as

$$\begin{bmatrix} \delta\dot{y}_1 \\ \delta\dot{y}_2 \\ \delta\dot{y}_3 \\ \delta\dot{y}_4 \end{bmatrix} = \begin{bmatrix} 0 & 1 & 0 & 0 \\ J_{21} - a_1 & J_{23} & 0 \\ 0 & 0 & 0 & 1 \\ J_{41} & 0 & J_{43} & -a_2 \end{bmatrix} \begin{bmatrix} \delta y_1 \\ \delta y_2 \\ \delta y_3 \\ \delta y_4 \end{bmatrix}, \tag{10}$$

where

$$\begin{aligned} J_{21} &= -b_1 - 3d_1 y_1^2 - e_1 y_3^2 - 2f_1 y_3 y_1, \\ J_{23} &= -\overline{C}_1 - 2e_1 y_3 y_1 - f_1 y_1^2 - 3g_1 y_3^2, \\ J_{41} &= -b_2 - 3g_2 y_1^2 - e_2 y_3^2 - 2f_2 y_3 y_1, \\ J_{43} &= -c_2 - 2e_2 y_3 y_1 - f_2 y_1^2 - 3d_1 y_3^2. \end{aligned}$$

From the definition in Ref. 21, the top Lyapunov exponent of the system is denoted as

$$\lambda = \lim_{t \to \infty} \frac{1}{t} \log \frac{\| \delta\boldsymbol{Y}(t) \|}{\| \boldsymbol{Y}(0) \|}. \tag{11}$$

It is noted that Eqs. (7) and (10) must be numerically solved simultaneously to acquire the largest Lyapunov exponent. The Runge–Kutta method of order 4 is adopted to solve Eqs. (7) and (10) simultaneously. In Eq. (7), there are several parameters, such as a_1, ..., g_2, F, Ω, and the flow velocity U, which can influence the chaotic motion of the system, except the initial conditions. The goal of the study is to detect whether or not the system of DWCNTs presents chaotic motion due to these parameters by determining the largest Lyapunov exponent of the system.

4. Numerical Results and Discussion

We consider the parameters E = 0.926 TPa, L = 60 nm, h = 0.34 nm, ρ = 1130 kg/m^3, ρ_f = 1000 kg/m^3, and R_1 = 2.5 nm. The damping coefficient ξ is considered as 0.1, and the initial conditions for T_1 and T_2 in Eqs. (5) and (6) are $T_1(0) = T_2(0) = 1$, and $\dot{T}_1(0) = \dot{T}_2(0) = 0$.

In Eqs. (5) and (6), there are several parameters that can influence the chaotic motion of the system, such as a_1, ..., g_1, a_2, ..., g_2, F, Ω, the velocity of the fluid, and the initial conditions.

The causes of the chaotic oscillations are mainly the geometric nonlinearity of the DWCNT, as determinied by inspecting Eqs. (5) and (6), particularly those of d_1, d_2, g_1, and g_2. The goal of the study is to detect whether or not these parameters cause the system of DWCNTs to present chaotic motion, by computing the top Lyapunov exponent of the system. This can be accomplished by changing one parameter while all the other parameters are fixed. First of all, we deal with the system having the parameters $F_0 = 1.0 \times 10^{-5}$ N/m and $\Omega = 1$. Here, Ω is the dimensionless driving frequency in Eq. (6). Then, we compute the top Lyapunov exponent of the DWCNT system by increasing the flow velocity from $U = 0.0$ to $U = 1.0 \times 10^{-3}$ m/s. The top Lyapunov exponent is presented versus the flow velocity U in Fig. 2. The top Lyapunov exponent is positive when the flow velocity is zero, namely, chaotic motion of the system occurs. However, when the flow velocity U increases to 5.2×10^{-4} m/s, the largest Lyapunov exponent changes from positive to negative, which implies that the motion of the DWCNTs has changed from chaotic to periodic. In Fig. 3, the Poincare map of DWCNTs is depicted for $U = 1.0 \times 10^{-4}$ m/s. As can be seen from the figure, the chaotic motion of the system is quite obvious. Now, for the same system except with the flow velocity U increased to $U = 1.0 \times 10^{-3}$ m/s, the largest Lyapunov exponent becomes negative as seen in Fig. 2. The Poincare map of DWCNTs is presented in Fig. 4. It is obvious that the motion of the system is periodic, as deduced from the figure. Therefore, the flow velocity U is very important in identifying whether or not the motion of the system is chaotic. To examine the effect of the driving frequency Ω on the chaotic behavior of the DWCNTs, we set the parameters $F_0 = 1.0 \times 10^{-5}$ N/m and $U = 1.0 \times 10^{-3}$ m/s and increase the driving frequency Ω from 1 to 30. In Fig. 5, the largest Lyapunov exponent becomes positive when the driving frequency Ω is larger than 5, namely, the motion of the system becomes chaotic. In Fig. 6, the Poincare map of DWCNTs is depicted. Obvious chaotic motion of the system is detected. Therefore, it is concluded that the driving frequency has a considerable influence on the chaotic feature of the DWCNTs. The final step is to examine the influence of load intensity on the chaotic behavior of the DWCNTs. We set the parameters $\Omega = 1$ and $U = 5.0 \times 10^{-4}$ m/s and increase the load intensity F_0 from 0 to 1.0×10^{-3} N/m. In Fig. 7, the largest Lyapunov exponent is negative when $F_0 = 0$, but it becomes positive with a slight

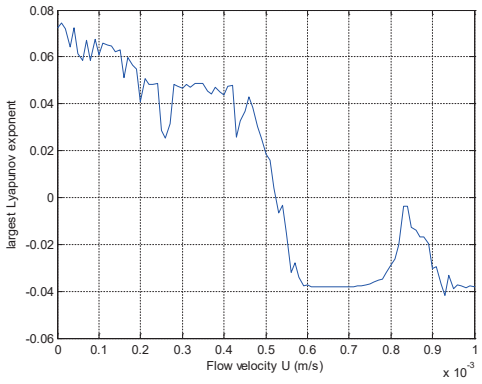

Fig. 2. (Color online) Largest Lyapunov exponent versus flow velocity U ($F_0 = 1.0 \times 10^{-5}$ N/m, $\Omega = 1$).

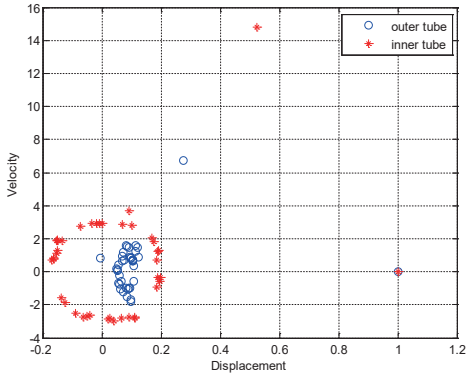

Fig. 3. (Color online) Poincare map of DWCNTs ($F_0 = 1.0 \times 10^{-5}$ N/m, $\Omega = 1$, $U = 1.0 \times 10^{-4}$ m/s).

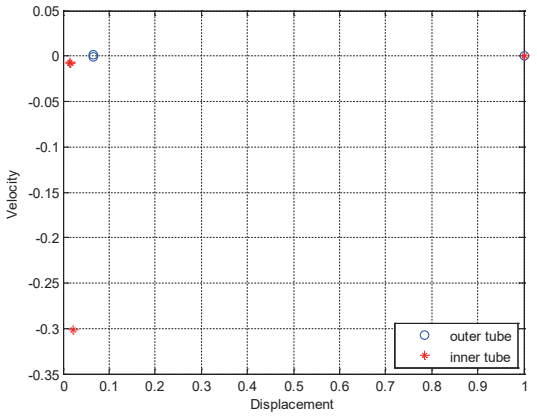

Fig. 4. (Color online) Poincare map of DWCNTs (F_0 = 1.0 × 10^{-5} N/m, Ω = 1, U = 1.0 × 10^{-3} m/s).

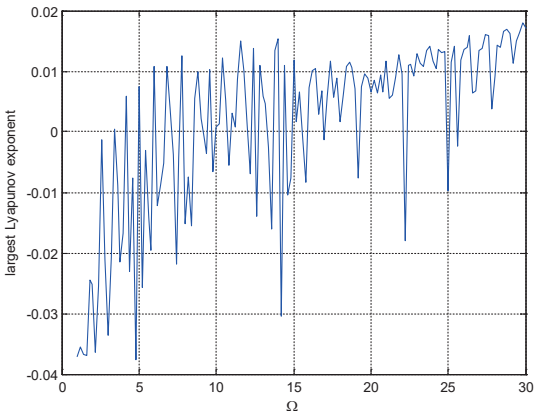

Fig. 5. (Color online) Largest Lyapunov exponent versus driving frequency Ω (F_0 = 1.0 × 10^{-5} N/m, U = 1.0 × 10^{-3} m/s).

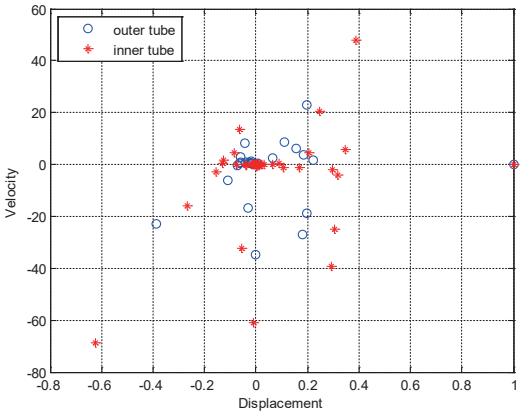

Fig. 6. (Color online) Poincare map of DWCNTs (F_0 = 1.0 × 10^{-5} N/m, Ω = 30, U = 1.0 × 10^{-3} m/s).

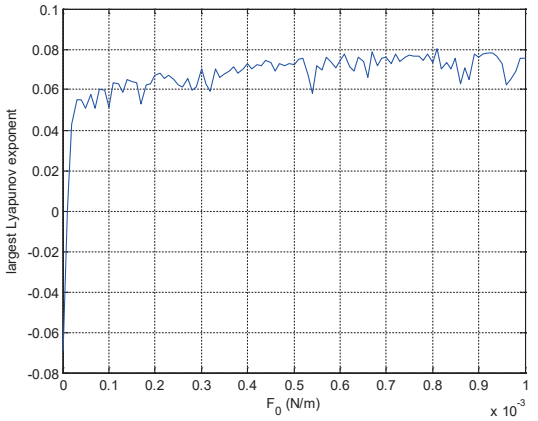

Fig. 7. (Color online) Largest Lyapunov exponent versus load intensity (Ω = 1, U = 5.0 × 10^{-4} m/s).

increase in F_0 and remains positive until F_0 = 1.0 × 10^{-3} N/m. In Fig. 8, the Poincare map of DWCNTs is given for F_0 = 1.0 × 10^{-6} N/m. Note that the periodic motion of the DWCNTs is observed because the top Lyapunov exponent is negative. For the load intensity F_0 increased to 1.0 × 10^{-3} N/m, the Poincare map of DWCNTs is shown in Fig. 9; chaotic motion of the DWCNTs is detected. On the basis of the aforementioned results, it is obvious that the flow velocity, driving frequency, and load intensity play important roles in the chaotic behavior of the system. In particular, it can be concluded that increasing the fluid velocity to a certain range will change the motion of the DWCNTs from chaotic to periodic; on the other hand, increasing the frequency or magnitude of external force to certain ranges will switch the motion of the DWCNTs from periodic to chaotic.

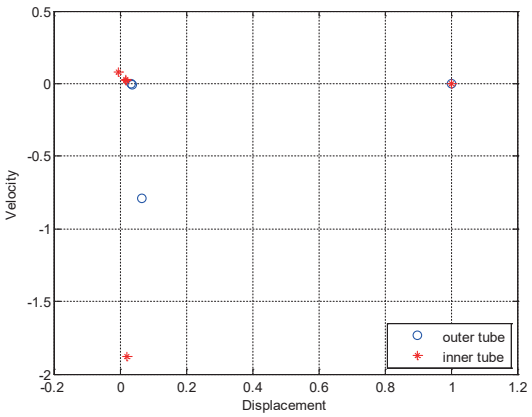

Fig. 8. (Color online) Poincare map of DWCNTs (F_0 = 1.0 × 10^{-6} N/m, Ω = 1, U = 5.0 × 10^{-4} m/s).

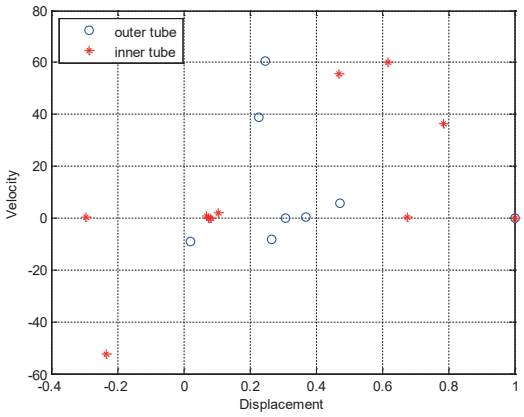

Fig. 9. (Color online) Poincare map of DWCNTs (F_0 = 1.0 × 10^{-3} N/m, Ω = 1, U = 5.0 × 10^{-4} m/s).

5. Conclusions

The chaotic behavior of DWCNTs with fluid was examined by studying the nonlinear characteristics. The governing equations of the system were derived and solved by the variation technique and Galerkin's method. Chaotic phenomena occurred when the top Lyapunov exponent of the coupled system changed from negative to positive. The calculations of the top Lyapunov exponent indicated that the chaotic motion of the nonlinear system occurred when the flow velocity U was between 0.0 and 5.2 × 10^{-4} m/s. When F_0 = 1.0 × 10^{-5} N/m and Ω = 1, the chaotic motion of the nonlinear DWCNT system switched to periodic motion on increasing the flow velocity to above 5.2 × 10^{-4} m/s. Moreover, the periodic motion of the nonlinear system switched back to chaotic motion on increasing the magnitude of the driving frequency Ω to above 25. In addition, when the amplitude of the applied load increased to F_0 = 1.0 × 10^{-3} N/m, the periodic motion of the DWCNTs switched back to chaotic motion. It can be concluded that these parameters play an important role in determining whether or not chaotic motion will occur in the system, and these parameters can be utilized to control the chaotic motion of the DWCNTs with fluid.

Acknowledgments

This study was sponsored by MOST in Taiwan under Grant No. MOST-105-2221-E-327-007-MY2. The author is thankful for the financial help.

References

1 S. Iijima: Nature **354** (1991) 56.
2 G. E. Gadd, M. Blackford, S. Moricca, N. Webb, P. J. Evans, A. M. Smith, S. Jacobsen, S. Leung, A. Day, and Q. Hua: Science **77** (1997) 933.

3 J. Liu, A. G. Rinzler, H. Dai, J. H. Hafner, R. K. Bradley, P. J. Boul, A. Lu, T. Iverson, K. Shelimov, C. B. Huffman, F. Rodriguez-Macias, Y.-S. Shon, T. R. Lee, D. T. Colbert, and R. E. Smalley: Science **280** (1998) 1253.
4 Y. Gao and Y. Bando: Nature **415** (2002) 599.
5 G. Hummer, J. C. Rasaiah, and J. P. Noworyta: Nature **414** (2001) 188.
6 W. Xia and L. Wang: Comput. Mater. Sci. **49** (2010) 99.
7 E. Ghavanloo, M. Rafiei, and F. Daneshmand: Phys. Lett. A **375** (2011) 1994.
8 T. P. Chang: Appl. Math. Modell. **36** (2012) 1964.
9 M. A. Hawwa and H. M. Al-Qahtani: Comput. Mater. Sci. **48** (2010) 140.
10 J. Yang, L. L. Ke, and S. Kitipornchai: Physica, E**42** (2010) 1727.
11 B. Fang, Y. X. Zhen, C. P. Zhang, and Y. Tang: Appl. Math. Modell. **37** (2013) 1096.
12 T. P. Chang: Microfluid. Nanofluid. **15** (2013) 219.
13 M. Simsek: Compos. Part B **56** (2014) 621.
14 Y. Z. Wang and F. M. Li: Mech. Res. Commun. **60** (2014) 45.
15 K. Kiani: Appl. Math. Modell. **37** (2013) 1836.
16 M. S. Siewe, H. Cao, and M. A. F. Sanjuan: Chaos, Solitons Fractals **39** (2009) 1092.
17 G. Litak, M. Borowiec, A. Syta, and K. Szabelski: Chaos, Solitons Fractals **40** (2009) 2414.
18 D. W. Huang, Q. Gao, H. L. Wang, J. F. Feng, and Z. W. Zhu: Chaos, Solitons Fractals **31** (2007) 242.
19 H. Norouzi and D. Younesian: Mech. Res. Commun. **69** (2015) 121.
20 A. Wolf, J. B. Swift, H. L. Swinney, and J. A. Vastano: Physica D **16** (1985) 285.
21 A. R. Zeni and J. A. C. Gallas: Physica D **89** (1995) 71.
22 K. Y. Xu, X. N. Guo, and C. Q. Ru: J. Appl. Phys. **99** (2006) 064303.

Appendix

$$a_1=\frac{1}{(M+m_1)\omega_0}\left[MU\left(\frac{\pi}{L}\right)^2\right],\quad b_1=\frac{1}{(M+m_1)\omega_0^2}\left[EI_1\left(\frac{\pi}{L}\right)^4-MU^2\left(\frac{\pi}{L}\right)^2+c_1\right],$$

$$\bar{C}_1=\frac{-c_1}{(M+m_1)\omega_0^2},\quad d_1=\frac{R_1^2}{(M+m_1)\omega_0^2}\left[\left(\frac{EA_1}{2L}+\frac{MU^2}{2L}\right)\left(\frac{\pi}{L}\right)^4-\frac{3}{8}MU^2\left(\frac{\pi}{L}\right)^2+\frac{3}{4}c_1\right],$$

$$e_1=\frac{9}{4}\frac{c_3R_1^2}{(M+m_1)\omega_0^2},\quad f_1=-\frac{9}{4}\frac{c_3R_1^2}{(M+m_1)\omega_0^2},\quad g_1=-\frac{3}{4}\frac{c_3R_1^2}{(M+m_1)\omega_0^2},$$

$$a_2=\frac{2\xi}{m_2\omega_0},\quad b_2=-\frac{c_1}{m_2\omega_0^2},$$

$$c_2=\frac{1}{m_2\omega_0^2}\left[E_2I_2\left(\frac{\pi}{L}\right)^4+c_1\right],\quad d_2=\frac{R_1^2}{m_2\omega_0^2}\left[\left(\frac{E_2A_2}{2L}\right)\left(\frac{\pi}{L}\right)^4+\frac{3}{4}c_3\right],$$

$$e_2=\frac{9}{4}\frac{c_3R_1^2}{m_2\omega_0^2},\quad f_2=-\frac{9}{4}\frac{c_3R_1^2}{m_2\omega_0^2},\quad g_2=-\frac{3}{4}\frac{c_3R_1^2}{m_2\omega_0^2},\quad F=\frac{2LF_0}{\pi m_2R_1\omega_0^2},\quad \Omega=\frac{\bar{\Omega}}{\omega_0}.$$